Respuestas, 23 (1) January - June 2018, pp. 13-18, ISSN 0122-820X

Respuestas
Journal of Engineering Sciences
RESPUESTAS

Original Article
https://doi.org/10.22463/0122820X.1324

Surface states and resonant states of Pd (111)

Estados de superficie y resonantes del Pd (111)

Hernán Javier Herrera-Suárez[a*], Alberto Rubio-Ponce[b], Rito Daniel Olguín-Melo[c]

[a*] *Doctor en Tecnología Avanzada, Universidad de Ibagué, Ibagué, Colombia. orcid.org/0000-0003-1273-7037*
[b] *Doctor en Física, Universidad Autónoma Metropolitana–Azcapotzalco, Ciudad de México, México. orcid.org/0000-0003-1158-7583*
[c] *Doctor en Física, Centro de Investigación y de Estudios Avanzados del Instituto Politécnico Nacional, Ciudad de México, México. orcid.org/0000-0003-3278-5159*

How to cite: H.J. Herrera-Suárez, A. Rubio-Ponce and R.D. Olguín-Melo, "Surface States and Resonant States of Pd (111)", *Respuestas,* vol. 23, no. 1, pp.13-18, 2018.

Received on July 23, 2017; Approved on November 15, 2017.

ABSTRACT

Keywords:
Bulk projected electronic band structure
Local density of states
Resonant states
Surface states

The motivation of this work is based on the importance of Palladium in processes such as catalysis and hence the need to know its electronic properties. We present a detailed study of the electronic structure of Palladium bands in the crystallographic direction (111). First we verify that the local density of states, projected in the volume, agrees with the results obtained for the case of the infinite medium previously reported. Next, a detailed study is made of different surface states and characteristic resonant states of the Palladium in the crystallographic direction (111). It was found that the results obtained are compared with the values published in the literature, and the prediction of different states not yet reported is made.

RESUMEN

Palabras Clave:
Estados de superficie.
Estados resonantes.
Estructura electrónica de bandas.

La motivación del presente trabajo se fundamenta en la importancia del Paladio en procesos de catálisis y sus propiedades electrónicas. En tal sentido, se presenta un estudio detallado de la estructura electrónica de bandas del Paladio en la dirección cristalográfica (111). De tal manera, se verificó que la densidad local de estados proyectada en el volumen, concordara con los resultados obtenidos para el caso del medio infinito previamente reportados, para ello, se realizó un estudio detallado de diferentes estados de superficie y estados resonantes característicos del Paladio en la dirección cristalográfica (111). Se halló que los resultados obtenidos se comparan con los valores publicados en la literatura, y se hizo la predicción de diferentes estados no reportados aún.

Introduction

Theoretically, the surface states can be calculated employing different methods: empirical and principled [1]-[3]. In that sense, a partial collection of the electronic structure of surfaces, surface states and resonant states, are reported in the Landolt-Börstein series [4].

Experimentally, the surface states occupied can be explored by ultraviolet photoemission spectroscopy determined in angle and the surface states unoccupied by inverse photoemission spectroscopy determined in angle [4].

The palladium is an important catalyst for rusting processes such as: methane catalytic rusting in gas turbines [5], hydrocarbon rusting and carbon rusts in exhaust pipes [6], which is particularly interesting due to high hydrogen solubility in the metal [7]-[10]. In the same order, it is considered as one of the best catalysts for the alkynes and dienes partial hydrogenation [11].

Moreover, the relation between the surface structure of the catalyst and the reaction activity or selectivity is an open question of interest from the technological and fundamental point of views.

For this reason, it is necessary a systematic study that explains the electronic characteristics of the palladium surfaces. In a recent research [12], the selective hydrogenation of acetylene through Pd nanoparticles with different shapes, concluded the catalyst that had Pd cube-shaped nanoparticles, which surface consisted of Pd structure (100), exhibited a higher acetylene conversion and ethylene selectivity than catalysts that had spherical nanoparticles, having a significant quantity of Pd nanoparticles (111).

However, the calculation of the functional density determined that in the Pd surface (111) there would be more ethylene activity and selectivity in contrast with the Pd surface (100) for acetylene hydrogenation [13].

In this research, a detailed analysis is done about the electronic structure of Pd bands (111), employing the strong link approximation and Green´s surface function coupling method. On the same hand, strong link Hamiltonians were built based on Slater Koster´s formalism (SK), in which the model

***Corresponding author.**
E-mail address: hernan.herrera@unibague.edu.co (Hernán Javier Herrera),

parameters, in the approximation of two centers, were taken from the manual charts of band electronic structures published by Papaconstantopoulos [14].

For the surface analysis (111), it was used the Green´s surface function coupling method and it was verified that the local density in states, reflected in the volume, agrees with the results obtained for the reference case [14]. Also, it was determined the type of symmetry of the wave functions that contributed to the surface states and resonant states of Pd (111), the obtained results were compared with the values published in the literature and the prediction is done about the different states that are not reported yet.

The present research was organized in the following way: The first section describes Green´s surface function coupling method deducing the expressions for the Green´s functions projected in the surface and the volume. The second section presents the projected volume bands, the dispersion of surface states and resonant states for the Pd in the crystallographic direction (111), there, it is compared the obtained results with the findings on the experimental and theoretical literature related. Finally, the third section is focused on the conclusions.

Theoretical Model

To do the calculation of the surface electronic properties is used the Green´s surface function coupling method (GFCM) [15], [16]. For the construction of Green´s surface function, it proceeds like this: With the Hamiltonian H of strong link it is defined a Green´s function associated like G, such that it satisfies the equation:

$$(\omega-H)G=I \tag{1}$$

In which H is the Hamiltonian of strong link, I is the unitary matrix and ω is the own energy value. A main layer is defined as the minimum group of atomic layers that reproduce the translational periodicity of the system carried out.

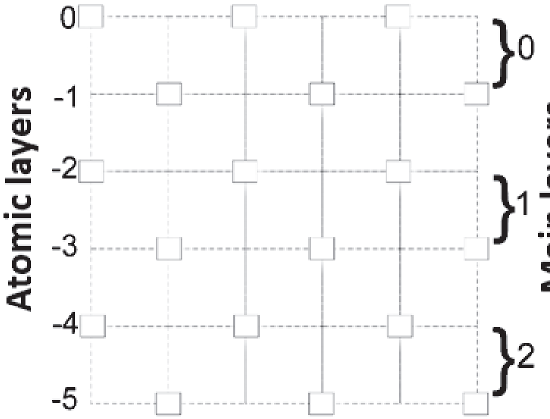

Figure 1. Main layer definition. It is observed that the atomic layers 0 and -1 create the first main layer (labeled with number 0), the atomic layers -2 and -3 create the second main layer (labeled with number 1) and the atomic layers -4 and -5 create the third main layer (labeled with number 2)

The main layer conventions are labeled with positive numbers and the atomic layers are labeled with negative numbers, and number zero is assigned to the surface atomic layer (figure 1). From this definition about the main layer, it is introduced the approximation of the GFCM method, which considers interactions in first neighbors among main layers. The quantity of atomic interactions will be determined by the number of atomic layers that define each main layer.

Being $|n\rangle$ the wave function associated with the ***n*** – th main layer. This wave function is a lineal combination of a certain number of atomic orbitals per atom in the unit cell, in our case the orbitals ***(s, p, d)***. Considering the space generated by the system of complete functions $|n\rangle$, it can be calculated the matrix elements of the equation (1). That space obtains:

$$[n \,|\, (\omega I-H)G \,|\, m]=\delta m,n^{\circ} \tag{2}$$

In the approximation of first neighbors among main layers, the identity operator is given as:

$$I= |n-1\rangle\langle n-1|+|n\rangle\langle n|+ |n+1\rangle\langle n+1| \tag{3}$$

Replacing the equation (3) in which the equation (2) obtains:

$$\delta m,n=(\omega-Hn,n)\ Gn,m - Hn,n -1\ Gn-1,m - Hn,n+1\ Gn+1,m \tag{4}$$

Where in this approximation and for the surface, n=0, we have H_(0,m)=0 for m≥2 (as in the strong link model the interactions are dominated by first neighbors interactions [17].

Then, the expression for Green´s function of surface projection will be:

$$Gs^{-1} = \varepsilon I - H0,0 - H0,1\ T \tag{5}$$

Meanwhile Green´s function for the volume projected in the first main layer will be [15], [16].

$$G_b^{-1}= G_s^{-1} - H_{1,0}\ T - \widetilde{H}_{0,1}T \tag{6}$$

Here, H0,0 and H0,1 are the interaction hamiltonians in intralayers and among main layers, respectively. To calculate these matrixes, it is needed to know the strong link matrixes of interaction among atomic layers (see details in references [18], [19]).

Then, T and $\widetilde{T}$ are the transfer matrixes, and they have all the data on surface electronic properties. These matrixes are coupled, this is why they cannot be evaluated exactly, so that they are developed in many iterative algorithms in order to obtain them numerically [19].

Due to the existence of a surface, the energetic states can differ from the states of inner parts of solids or their volume; if the surface states which energy value and wave vector coincide with the inner states of the solid, they are nominated resonant states [18]. The surface states which energy value and wave vector do not coincide with any inner state of the solid are nominated surface states [20]. These have wave functions that buffer themselves exponentially at the same time that they enter the crystal.

The surface states are located in the energetic breaches of the volume bands structure and emerge due to the break of the crystal symmetry. Finally, once we know the differences of Green´s function mentioned beforehand, it can be calculated the surface states and the resonant states directly from the poles from the real part of Green´s function, whereas from the imaginary part we can find the density of local states [15], [16].

Results and discusion

Density of States Figure number 2 shows volume states density of the Pd applying the reference parameters [14], that are related to the model through energy integrals for the crystal in terms of integrals of two centers [21]. Figure 2b exhibits the local density of states projected on the surface (dotted red line) and the local states density projected on the volume (solid black line) for the Pd (111).

In figures 2a and 2b, the zero of the energy axis represents the Fermi level (EF). For calculating figure 2b there were used 136 points in the irreducible segment of the first Brillouin zone [22] (the number of the extracted points reproduces the most significant features of the local density of volume states and optimize the time of calculation).

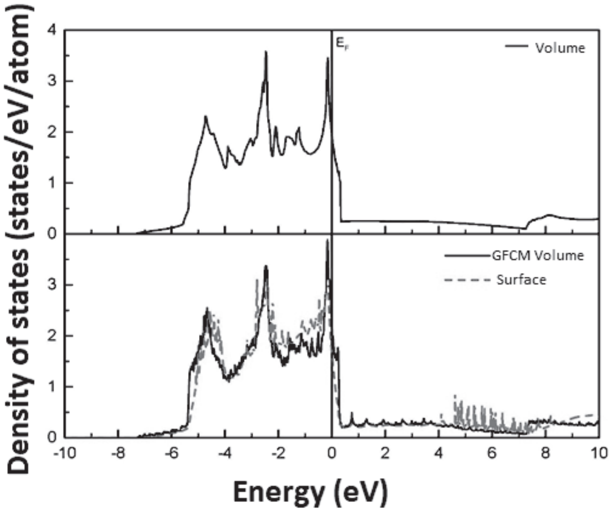

Figure 2. (a) Density of states of Pd volume applying the reference parameters [14] (b) Local Density of States (DLE) of volume (continue line) and surface (discontinued line) of Pd (111), which are obtained with the MAFG method. Fermi level is found in the origin

A direct comparison on the local density of states projected on the volume, with the states density reported in the reference [14], allows to observe that the calculation properly reproduces the main features of the density of states. In this respect, the local density of volume states that is calculated using the MAFG, is adequately compared for energies below the Fermi level, where are localized three spikes in the energies of: -4.66, -2.46 and -0.16 eV, which differ of the reported ones in the reference [14], in 0.0748, 0.0162 and 0.01034 eV.

On the basis of these facts, it is shown that the surface electronic band structure coincides with the reported results [14].

The partial contributions of atomic orbitals ***s, p*** y ***d*** to the local density of Pd states (111), are shown in figure 3. Particularly, figure 3c shows that the approximate energy rate is -5.42 eV a 0.44 eV, the main contribution of local density is obtained from electrons Pd - 5d, in contrast with the contributions of the orbitals ***s y p*** (see figures 3a and 3b).

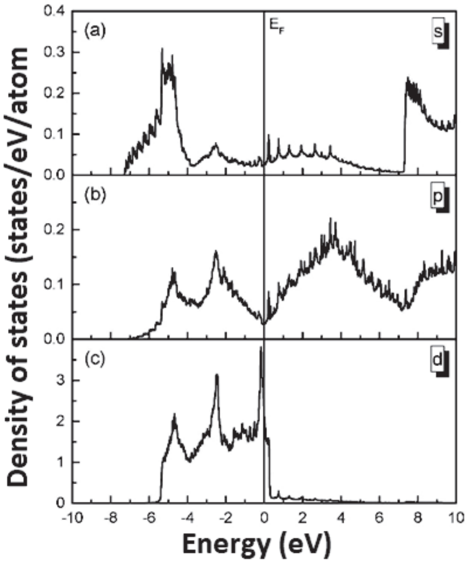

Figure 3. Partial contributions of the atomic orbitals (a) (b) (c) to the Pd local density of states (111), obtained from the GCFM method. The Fermi level is found in the origin

Projected bands of volume, surface states and resonant states of Pd (111). The measured values of the surface states (solid black circles) and the measured resonant states (white circles), as well as the projected bands of surface volume (111), are shown in figure 4.

The electronic features of these states are respectively shown in tables I and II. According to the calculations, there have been obtained ten surface states and four resonant states. Regarding the electronic and symmetry characteristics found for the different surface states and resonant states, it is had:

The state Es1 does not present dispersion and it is located in 3.48 eV below Fermi level as it is observed in figure 3, in 0.05 $|\overline{K}\,\overline{\Gamma}|$, being located in an energetic breach, and its width in the $\overline{K}$ point from the two-dimensional Brillouin zone is 0.47 eV, in which the kind of symmetry of the wave function that contributes to this state is $d_{3z^2} - r^2$.

Theoretically, this state has been identified in the references [10] and [23], results that differ from the current research in 0.01 and 0.54 eV, respectively.

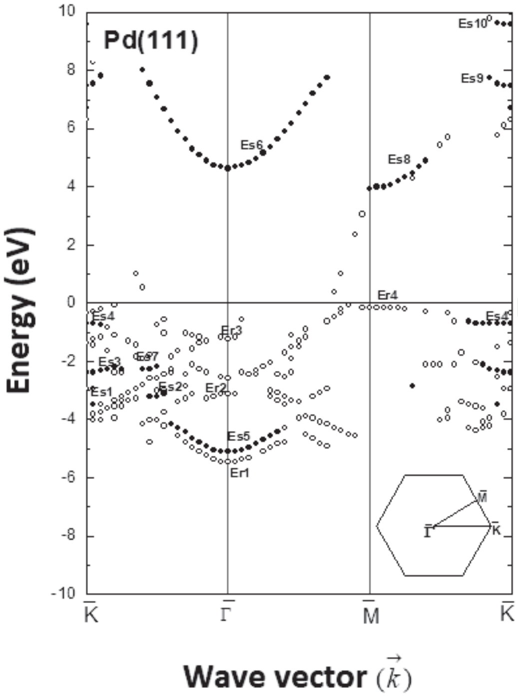

Figure 4. Volume bands structure projected from Pd (111) calculated with the GFCM method. The black and white circles represent the surface states and the resonant states, respectively. The Fermi level is found in the origin

The surface state is Es$_2$ in approximately -3.21 eV in 0.45 $|\overline{K}\,\overline{\Gamma}|$ and it scatters until -3.14 eV in 0.55 $|\overline{K}\,\overline{\Gamma}|$, being located in an energetic breach which width is 0.20 eV in 0.50 $|\overline{K}\,\overline{\Gamma}|$, being the result of the hybridization of atomic orbitals d_{xy}. Experimentally and theoretically, this state has not been identified.

The surface state Es$_3$ starts from -2.12 eV in 0.80 $|\overline{M}\overline{K}|$, crosses point $\overline{K}$ in -2.39 eV, approximately, and disperses to -2.25 eV en 0.25 $|\overline{K}\,\overline{\Gamma}|$, being in an energetic breach whose width is 1.08 eV in $\overline{K}$, and whose orbital character is d.

Theoretically, this state has been identified in the references [10] and [23], results that differ from our result in 0.22 eV.

The surface state Es$_4$ starts from -0.62 eV in 0.70 $|\overline{M}\overline{K}|$, crosses point $\overline{K}$ in -0.69 eV, approximately, and disperses to -0.76 eV en 0.10 $|\overline{K}\,\overline{\Gamma}|$, being in an energetic breach whose width is 0.68 eV in $\overline{K}$, in which the kind of symmetry of the wave function that contributes to this state is $d_{3z^2-r^2}$. Theoretically, this state has been identified in the references [10] and [23], results that differ in 0.62 y 0.38 eV with our results.

Table I. Surface states of Pd (111). The first column represents the surface state; the second one the wave vector in which it is located the state, in units [π/a]; the third one the value of its energy obtained by experimental techniques, in units [eV]; the fourth one the value of its energy obtained by theoretical methods, in units [eV]; the fifth one shows the value of its energy obtained in our calculation, in units [eV], and the last column shows the kind of symmetry of wave functions that contribute to the state according to our calculation

Es	$\vec{k}\left(\frac{\pi}{a}\right)$	$E_{exp}(eV)$	$E_{teórico}\ (eV)$	$E_{NC}\ (eV)$	SFO_{NC}
Es1	$\left(\frac{19}{15}\sqrt{2},0\right)$		−3.49 [10] −2.94 [23]	−3.48	$d_{3z^2-r^2}$
Es2	$\left(\frac{11}{15}\sqrt{2},0\right)$			−3.21	d_{xy}
Es3	$\left(\frac{4}{3}\sqrt{2},0\right)$		−2.34 [10] −1.90 [23]	−2.39	d
Es4	$\left(\frac{4}{3}\sqrt{2},0\right)$		−1.24 ([10] −1.00 [23]	−0.69	$d_{3z^2-r^2}$
Es5	(0,0)		−5.09 [10] −4.00 [23]	−5.11	$s, d_{3z^2-r^2}$
Es6	(0,0)	1.7 [24]	1.8 [23]	4.61	s, p_z
Es7	$\left(\frac{11}{15}\sqrt{2},0\right)$			−2.25	$d_{xy,yz,zx}$
Es8	$\left(\sqrt{2},\frac{\sqrt{6}}{3}\right)$			3.93	s, p_{xy}
Es9	$\left(\frac{4}{3}\sqrt{2},0\right)$			7.46	p_{xy}
Es10	$\left(\frac{4}{3}\sqrt{2},0\right)$			9.57	p_{xy}

Theoretically, this state has been identified in the references [10] and [23], results that differs in 0.62 and 0.38 eV with our results.

The surface state Es$_5$ starts from -4.16 eV in 0.60 $|\overline{K}\,\overline{\Gamma}|$, crossing the $\overline{\Gamma}$ point in -5.11 eV, approximately, and it is scattered in a parabolic form until -4.33 eV in 0.35 $|\overline{\Gamma}\,\overline{M}|$, being located in an energetic breach which width is 2.10 eV in $\overline{\Gamma}$, being the result of hybridization of atomic orbitals s, $d_{3z^2-r^2}$. Theoretically, this state has been identified in the references [10] and [23], result that differs in 0,06 and 1.15 eV, respectively with the results of the current article.

The surface state Es$_6$ starts from 8.42 eV in 3.35 $|\overline{K}\,\overline{\Gamma}|$, and disperses to -7.74 eV en 0.70 $|\overline{\Gamma}\overline{M}|$, being in an energetic breach whose width is 6.59 eV in $\overline{\Gamma}$, and whose orbital character is *s,p_z.* This state has been identified experimentally in the reference [24] and theoretically in the reference [23], results that differ in 2.91 eV and 2.81 eV, respectively. A possible explanation for the error found in the energies of the states Es$_3$, Es$_4$ and Es$_6$, may be the fact that our calculation has considered an ideal surface. A correction to this approach should include the effects of reconstruction and relaxation of the surface, effects that remain pending.

The surface state Es$_7$ starts from -2.25 eV in 0.40 $|\overline{K}\,\overline{\Gamma}|$ and it is scattered until -2.19 eV in 0.50 $|\overline{K}\,\overline{\Gamma}|$, in which the kind of symmetry of the wave functions that contribute to this state are dxy, yz, zx, finding themselves in the same energetic breach than the state Es$_3$.

The surface state Es$_8$ starts from 3.93 eV in $\overline{M}$ and it is scattered until 4.88 eV in 0.40 $|\overline{M}\overline{K}|$, finding itself in an energetic breach which width is 3.40 eV in *M*, being the result of hybridization of atomic orbitals *s, px,y*.

and D2 from/on/in Pd (111)", *Surface Science,* vol. 90, pp. 162-180, 1979.

[10] W. Dong and J. Hafner, "H2 dissociative adsorption on Pd (111)", *Physical Review B*, vol. 56, pp. 15396–15403, 1997.

[11] J.S. Zhu and Y.S. Shon, "Mechanistic interpretation of selective catalytic hydrogenation and isomerization of alkenes and dienes by ligand deactivated Pd nanoparticles", *Nanoscale,* vol. 7, pp. 17786-17790, 2015.

[12] S.K. Kim, C. Kim and J.H. Lee, "Performance of shape-controlled Pd nanoparticles in the selective", *Journal of Catalysis,* vol. 306, pp. 146-154, 2013.

[13] B. Yang, R. Burch and C. Hardacre, "Influence of surface structures, subsurface carbon and hydrogen, and surface alloying on the activity and selectivity of acetylene hydrogenation on Pd surfaces: A density functional theory study", *Journal of Catalysis,* vol. 305, pp. 264–276, 2013.

[14] D.A. Papaconstantopoulos, Handbook of the band structure of elemental solids, New York: Plenum Press, 1986, pp. 234-238.

[15] F. Garcia-Moliner and V.R. Velasco, Theory of Single and Multiple Interfaces, London: World Scientific, 1992, pp. 323-336.

[16] F. Garcia-Moliner and V.R Velasco, "Theory of incomplete crystals, surfaces, defects, interfaces and layered structures", *Progress in Surface Science,* vol. 21, no. 2, pp. 93-162, 1986.

[17] C.Z. Wang, W.C. Lu and Y.X. Yao, "Tight-binding Hamiltonian from first-principles", *Science Modeling Simulation,* vol. 15, pp. 81–95, 2008.

[18] M.M. Lannoo, Atomic and electronic structure of surfaces: theoretical foundations, Berlin, 1991: *Springer-Verlag,* vol 16, pp. 10-13, 1991.

[19] M.P. Lopez Sancho, J.M. Lopez Sancho and J. Ru, "Quick iterative scheme for the calculation of transfer matrices: application to Mo (100)", *Journal of Physics F: Metal Physics,* vol. 14, pp. 1205- 1215, 1984.

[20] P.V. Pavlov and A.F. Jojlov, Física del estado sólido, Moscú: MIR, 1987, pp. 270.

[21] J.C. Slater and G.F. Koster, "Simplified LCAO Method for the Periodic Potential Problem", *Physical Review,* vol. 1524, pp. 1458, 1954.

[22] D.J. Chadi and M.L. Cohen, "Special Points in the Brillouin Zone", *Physical Review B,* vol. 8, pp. 5747-5753, 1973.

[23] S.G. Louie, "Electronic states and adsorbate induced photoemission structure on the Pd (111) surface", *Physical Review Letters*, vol. 40, pp. 1525-1528, 1978.

[24] P.D. Johnson and N.V. Smith, "Inverse photoemission observation of an unoccupied surface state on Pd (111)", *Physical Review Letters,* vol. 49, pp. 290-292, 1982.